Sub-wavelength grating mode transformers in silicon slab waveguides

Przemek J. Bock[1,2]*, Pavel Cheben[1], Jens H. Schmid[1], André Delâge[1], Dan-Xia Xu[1], Siegfried Janz[1], Trevor J. Hall[2]

[1]*Institute for Microstructural Sciences, National Research Council Canada, Ottawa, Canada*
[2]*Centre for Research in Photonics, University of Ottawa, Ottawa, Canada*
**przemek.bock@nrc.ca*

Abstract: We report on several new types of sub-wavelength grating (SWG) gradient index structures for efficient mode coupling in high index contrast slab waveguides. Using a SWG, an adiabatic transition is achieved at the interface between silicon-on-insulator waveguides of different geometries. The SWG transition region minimizes both fundamental mode mismatch loss and coupling to higher order modes. By creating the gradient effective index region in the direction of propagation, we demonstrate that efficient vertical mode transformation can be achieved between slab waveguides of different core thickness. The structures which we propose can be fabricated by a single etch step. Using 3D finite-difference time-domain simulations we study the loss, polarization dependence and the higher order mode excitation for two types (triangular and triangular-transverse) of SWG transition regions between silicon-on-insulator slab waveguides of different core thicknesses. We demonstrate two solutions to reduce the polarization dependent loss of these structures. Finally, we propose an implementation of SWG structures to reduce loss and higher order mode excitation between a slab waveguide and a phase array of an array waveguide grating (AWG). Compared to a conventional AWG, the loss is reduced from −1.4 dB to < −0.2 dB at the slab-array interface.

OCIS codes: (130.3120) Integrated optics devices; (230.1950) Diffraction gratings; (060.1810) Buffers, couplers, routers, switches, and multiplexers.

References and links

1. S. M. Rytov, "Electromagnetic properties of a finely stratified medium," Sov. Phys. JETP **2**, 466–475 (1956).
2. P. Lalanne, and J.-P. Hugonin, "High-order effective-medium theory of subwavelength gratings in classical mounting: application to volume holograms," J. Opt. Soc. Am. A **15**(7), 1843–1851 (1998).
3. H. Kikuta, H. Toyota, and W. Yu, "Optical elements with subwavelength structured surfaces," Opt. Rev. **10**(2), 63–73 (2003).
4. C. F. R. Mateus, M. C. Y. Huang, L. Chen, C. J. Chang-Hasnain, and Y. Suzuki, "Broad-band mirror (1.12–1.62 μm) using a subwavelength grating," IEEE Photon. Technol. Lett. **16**, 1676–1678 (2004).
5. P. Cheben, D.-X. Xu, S. Janz, and A. Densmore, "Subwavelength waveguide grating for mode conversion and light coupling in integrated optics," Opt. Express **14**(11), 4695–4702 (2006).
6. P. Cheben, S. Janz, D.-X. Xu, B. Lamontagne, A. Delâge, and S. Tanev, "Highly efficient broad-band waveguide grating coupler with a sub-wavelength grating mirror,", in *Frontiers in planar lightwave circuit technology*, S. Janz et al., eds. (Springer, 2006), 235–243.
7. R. Halir, P. Cheben, S. Janz, D.-X. Xu, I. Molina-Fernández, and J. G. Wangüemert-Pérez, "Waveguide grating coupler with subwavelength microstructures," Opt. Lett. **34**(9), 1408–1410 (2009).
8. J. H. Schmid, P. Cheben, S. Janz, J. Lapointe, E. Post, and D.-X. Xu, "Gradient-index antireflective subwavelength structures for planar waveguide facets," Opt. Lett. **32**(13), 1794–1796 (2007).
9. J. H. Schmid, P. Cheben, S. Janz, J. Lapointe, E. Post, A. Delâge, A. Densmore, B. Lamontagne, P. Waldron and D.-X. Xu, "Subwavelength grating structures in silicon-on-insulator waveguides," Advances in Optical Technologies: Special Issue on Silicon Photonics, 2008, Article ID 685489, doi:10.1155/2008/685489 (invited), (2008).

#112127 - $15.00 USD Received 1 Jun 2009; revised 13 Aug 2009; accepted 15 Aug 2009; published 8 Oct 2009

10. P. Cheben, "Wavelength dispersive planar waveguide devices: echelle gratings and arrayed waveguide gratings," in *Optical waveguides: from theory to applied technologies*, M. L. Calvo and V. Lakshminarayanan, eds. (CRC Press, 2007), 173–230.
11. P. Cheben, A. Delâge, S. Janz, and D.-X. Xu, "Echelle gratings and arrayed waveguide gratings for WDM and spectral analysis," in *Advances in information optics and photonics*, A.T. Friberg and R. Dändliker, eds. (SPIE Press, 2008), 599–632.
12. C. R. Doerr, and K. Okamoto, "Advances in silica planar lightwave circuits," J. Lightwave Technol. **24**(12), 4763–4789 (2006).
13. X. J. M. Leijtens, B. Kuhlow, and M. K. Smit, "Arrayed waveguide gratings," in *Wavelength filters in fiber optics*, H. Venghaus, (Springer Verlag, 2006), 125–187.
14. P. Cheben, A. Delâge, A. Densmore, M. Florjanczyk, S. Janz, B. Lamontagne, J. Lapointe, E. Post, J. Schmid and D.-X. Xu, "Silicon photonic waveguide structures and devices: From fundamentals to implementations in spectroscopy and biological sensing," NATO Advanced Study Institute, (Springer 2009).
15. P. Cheben, J. H. Schmid, A. Delâge, A. Densmore, S. Janz, B. Lamontagne, J. Lapointe, E. Post, P. Waldron, and D.-X. Xu, "A high-resolution silicon-on-insulator arrayed waveguide grating microspectrometer with sub-micrometer aperture waveguides," Opt. Express **15**(5), 2299–2306 (2007).
16. Y. Komai, H. Nagano, K. Okamoto, and K. Kodate, "Spectroscopic sensing using a visible arrayed-waveguide grating," Proc. SPIE **5867**, 91–102 (2005).
17. J.-J. He, E. S. Koteles, B. Lamontagne, L. Erickson, A. Delâge, and M. Davies, "Integrated polarization compensator for WDM waveguide demultiplexers," IEEE Photon. Technol. Lett. **11**(2), 224–226 (1999).
18. P. Cheben, D.-X. Xu, S. Janz, A. Delâge, and D. Dalacu, "Birefringence compensation in silicon-on-insulator planar waveguide demultiplexers using a buried oxide layer," Proc. SPIE **4997**, 181–189 (2003).
19. P. J. Bock, P. Cheben, A. Delâge, J. H. Schmid, D.-X. Xu, S. Janz, and T. J. Hall, "Demultiplexer with blazed waveguide sidewall grating and sub-wavelength grating structure," Opt. Express **16**(22), 17616–17625 (2008).
20. S. Y. Chou, P. R. Krauss, and P. J. Renstrom, "Imprint lithography with 25-nanometer resolution," Science **272**(5258), 85–87 (1996).
21. P. Cheben, J. H. Schmid, P. J. Bock, D.-X. Xu, S. Janz, A. Delâge, J. Lapointe, B. Lamontagne, A. Densmore, and T. Hall, "Sub-wavelength nanostructures for engineering the effective index of silicon-on-insulator waveguides," presented at the 11th International Conference on Transparent Optical Networks, Azores, Portugal, June 28 - July 2, 2009.
22. J. H. den Besten, M. P. Dessens, C. G. P. Herben, X. J. M. Leijtens, F. H. Groen, M. R. Leys, and M. K. Smit, "Low-loss, compact, and polarization independent phasar demultiplexer fabricated by using a double-etch process," IEEE Photon. Technol. Lett. **14**(1), 62–64 (2002).
23. Y. P. Li, "Optical device having low insertion loss," Patent 5745618 (1998).

1. Introduction

Light propagation in a sub-wavelength structured medium can be described by the effective medium theory [1,2], according to which different materials combined at a sub-wavelength scale can be approximated as a homogeneous effective medium. Sub-wavelength gratings (SWGs) have been known and used for many years [3], commonly as an alternative to antireflective (AR) coatings on bulk optical surfaces. Recently, various interesting SWG structures have been proposed, including SWG mirrors [4], microphotonic fiber-chip couplers [5] and off-plane chip couplers [6,7]. Anti-reflective and mirror structures at chip facets have also been developed using both gradient index (GRIN) and interference effects [8,9]. Here we propose several mode transformer designs exploring the GRIN effect in SWG waveguide structures for mode transformation in waveguides of different geometries. By creating the adiabatic GRIN waveguide region in the direction of propagation, we demonstrate that mode size transformation is readily achieved in structures that can be fabricated using a single etch step. Our mode transformers are designed for minimal mode mismatch loss and coupling to higher order modes, specifically aiming at applications in silicon-on-insulator (SOI) wavelength multiplexers.

Wavelength (de)multiplexers [10–13] based on arrayed waveguide gratings (AWGs) and echelle gratings have been developed for Wavelength Division Multiplexed (WDM) communication networks, with new applications emerging, particularly in spectroscopy and sensing [14–16]. Devices have progressively been made smaller, resulting in higher integration density, more functionalities on a single chip, greater yields and lower cost. In particular, the high index contrast of the SOI platform allows for waveguides of sub-micrometer dimensions and waveguide bend radii as small as a few micrometers, thereby markedly reducing device size. However, coupling loss between waveguides of different geometries is increased due to

#112127 - $15.00 USD Received 1 Jun 2009; revised 13 Aug 2009; accepted 15 Aug 2009; published 8 Oct 2009

the high index contrast. For example, polarization independence of AWGs and echelle gratings can be achieved using etched polarization compensation regions [17] resulting in a mode mismatch at the compensator interface. The mode mismatch loss can be reduced using a polarization compensator with a buried oxide layer [18], but this requires deposition of additional optical layers, thus adding fabrication complexity. In another application, a sidewall grating as a demultiplexer has been studied with benefits including very compact footprint, reduced effect of sidewall roughness on crosstalk and direct control of amplitude and phase of the diffracted field [19]. To reduce out-of-plane radiation losses, a shallow trench between the grating and the combiner slab is used. Still, a loss penalty arises at the interface between the shallow trench and the slab output combiner region. Both cases (polarization compensator and shallow trench in curved waveguide demultiplexer) include coupling between two slab waveguides of different core thicknesses. In the case of the polarization compensator, a SWG transition region can be used at the boundary between of the etched compensator slab to reduce mode mismatch loss. Subwavelength grating at the interface of a trench in a slab waveguide (like in [19]) can be use to similar effect. In this paper we will show that loss at the junction between two waveguides of different core thickness can be reduced by using a SWG GRIN region in the direction of propagation, to adiabatically modify the vertical mode confinement. The SWG region results in a gradual change from the effective index of the thick slab waveguide to the thin slab waveguide.

In particular, we propose two types of mode converters, i.e. based on triangular (1D grating) and triangular-transverse (2D grating) SWG structures that can be fabricated using a single etch step. Our 3D finite-difference time-domain (FDTD) simulations indicate a significant improvement over a conventional geometry for various waveguide core dimensions, including Si cores of sub-micrometer thickness. We also propose two possible solutions for mitigating polarization dependent loss (PDL) of these SWG mode transformers by using a partial transverse SWG and SWG structures in the region between the triangular teeth. Finally, we propose and evaluate a SWG between the slab waveguide and the phase array of a photonic wire array waveguide grating. This grating forms a transition region, adiabatically matching the effective index of the slab waveguide with the phase array. Simulation results (3D FDTD) show that both loss and higher order mode excitation are significantly reduced using SWG structures.

The devices presented in this paper are intended for fabrication using electron beam lithography, with low cost fabrication possible using nano-imprinting [20]. Minimum feature size for these devices is 50 nm, which can be increased to 100 nm without significant penalty provided the same effective index change is maintained with the larger feature size. Initial fabrication results are described in [8,21] and are promising.

2. Mode Transformer Principle

According to effective medium theory, different optical materials combined at a sub-wavelength scale, can be approximated by an effective homogeneous material [2]. Within this approximation, an effective medium can be characterized by an effective index defined as a power series of the homogenization parameter $\chi = \Lambda/\lambda$, where Λ is the grating pitch and λ is the wavelength of light. Provided the pitch Λ is less than the 1st order Bragg period $\Lambda_{Bragg} = \lambda/(2n_{eff})$, the grating is sub-wavelength and diffraction effects are frustrated. For the SOI waveguide platform, the two obvious choices for the high and low index materials to create the effective medium are silicon (waveguide core) and silica (cladding). A gradual change in the ratio of Si to SiO_2 along the light propagation direction (Fig. 1, z-axis) results in a corresponding effective index change of the composite medium. We propose to use this principle to create a transition region (*T*, Figs. 1(b) and 1(c)) between two slab waveguides (*A* and *B*, Figs. 1(b) and 1(c)) of different thicknesses or a slab waveguide and a waveguide array (Fig. 1(d)). In the following analysis we study these structures using 3D FDTD simulations. In particular, we focus on reducing loss, higher order mode excitation and PDL of these structures.

#112127 - $15.00 USD Received 1 Jun 2009; revised 13 Aug 2009; accepted 15 Aug 2009; published 8 Oct 2009

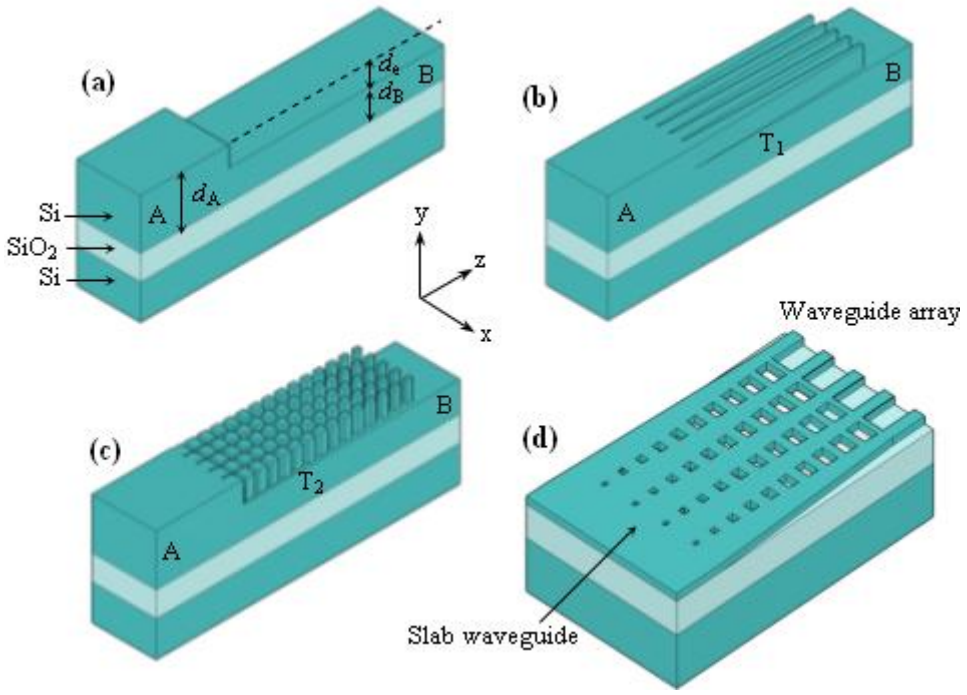

Fig. 1. 3D schematics of junctions between two waveguides of different geometries, with: a) conventional single step interface, b) 1D grating, triangular SWG transition region, and c) 2D grating, triangular-transverse SWG transition region. d) SWG structure at the boundary between slab waveguide and a waveguide array.

3. Design and Simulation

3.1 SWG transition between slab waveguide of different core thicknesses

We compare three geometries of mode transformers between slab waveguides of different core thicknesses: the conventional single-step (Fig. 1(a)), the triangular SWG transition region (T_1, Fig. 1(b)) and the triangular-transverse transition region (T_2, Fig. 1(c)). For the conventional single-step, the simulation was performed for an initial slab of a thickness d_A and a length of 2 μm, followed by a 20 μm long thinner slab waveguide *B*. This conventional structure (an abrupt effective index mismatch) is a benchmark design for assessing our SWG designs. Our first SWG mode transformer design employs triangular SWG structures (Fig. 2(a)) with length 20 μm and pitch 0.3 μm, to create a GRIN effect similar to the anti-reflective structure we reported in [8]. The structure length was chosen as a compromise between simulation time demands and ensuring an adiabatic mode transition between the different slab waveguide thicknesses. Our second design, a SWG triangular-transverse mode transformer (Fig. 2(b)) has the triangular structures identical to the first structure, but with a transverse SWG added. The geometrical parameters of these transverse gratings are Λ_i = 180 nm, Λ_f = 220 nm, a_i = 130 nm and a_f = 50 nm, where Λ_i and Λ_f are the initial and final grating pitch and a_i and a_f are the initial and final Si segment lengths (Fig. 2(b)). These grating parameters ensure suppressed diffraction and a gradual transition from the initial slab waveguide to the thinner slab waveguide. Here the sub-wavelength transverse grating duty ratio $r(z) = a(z)/\Lambda(z)$ decreases along the light propagation direction, as we proposed in [5] to ease the transition.

#112127 - $15.00 USD Received 1 Jun 2009; revised 13 Aug 2009; accepted 15 Aug 2009; published 8 Oct 2009

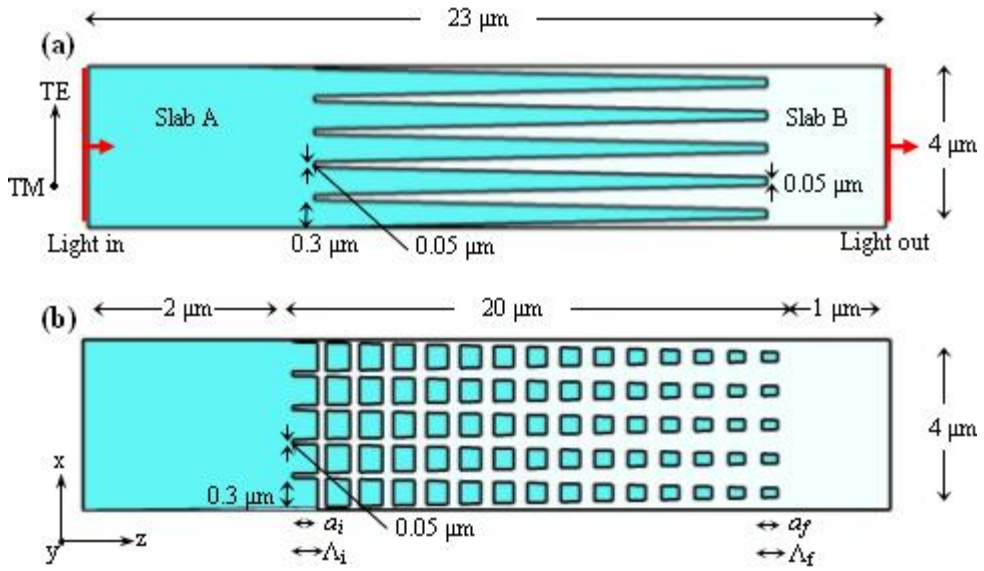

Fig. 2. Top view of mode transformer. a) Triangular SWG structure; b) Triangular-transverse SWG structure. 3D FDTD simulations were performed for both structures for three different thicknesses of slab waveguide *A*: d_A = 0.5 μm, 1.0 μm and 1.5 μm, with variable etch depth (d_A-d_B).

3D FDTD simulations were performed for a layout size of $x \times y \times z = 4 \times 4 \times 24$ μm^3 on the SOI waveguide platform with material refractive indexes n_{Si} = 3.476 and n_{SiO2} = 1.444 (SiO_2 cladding). Mesh size used for the simulations was $\Delta x \times \Delta y \times \Delta z = 20 \times 20 \times 20$ nm^3, while the time step $\Delta t = 3.3 \times 10^{-17}$ s was set according to the Courant limit. For each design (conventional single-step, triangular SWG and triangular-transverse SWG), three initial slab waveguide (*A*) thicknesses of d_A = 0.5 μm, 1.0 μm and 1.5 μm were evaluated. For each slab waveguide thickness, simulations were run for several etch depths $d_e = d_A - d_B$. The mode mismatch loss of each design was calculated as the power coupled to the fundamental mode of the thinner slab waveguide (*B*). All simulations were performed by exciting a continuous wave (CW) initial slab fundamental mode at wavelength λ = 1.54 μm.

Using a first order effective medium theory approximation, an initial model of the upper cladding transition region for a triangular SWG is done similar to [8]. Due to the form birefringence of the triangular SWG structure, the first order effective medium theory approximation of the SWG transition will be polarization dependent. Figure 3 shows effective medium index change from Si (position z = 0 μm) to SiO_2 (position z = 20 μm) as a function of position for TE and TM polarization. From this estimate, it is evident that for TM polarization the effective medium index change is more adiabatic then for TE polarization.

Length dependence for a triangular SWG structure was assessed using 3D FDTD simulations for 5 μm, 10 μm and 20 μm long structures with d_A = 1.0 μm and d_e = 0.4 μm (40% etch). Figure 4 shows loss as a function of triangular SWG length, indicating reduced loss for longer structures. As predicted by the effective medium theory approximation (Fig. 3), TM polarization has lower loss compared to TE polarization due to the superior TM adiabaticity. Longer triangular SWG lengths could not be assessed (though are expected to have further reduced loss) due to excessive simulation duration. In all our subsequent simulations we used 20 μm long structures.

3D FDTD simulations were also used to assess the taper waveguide with a gradually changed thickness from 1.0 μm to 0.6 μm, over 20 μm. The calculated TE loss was –1.7 dB and TM loss –1.2 dB. This is a higher loss than for our optimal SWG structures, which seems

#112127 - $15.00 USD Received 1 Jun 2009; revised 13 Aug 2009; accepted 15 Aug 2009; published 8 Oct 2009

counterintuitive. This loss penalty appears to be a numerical artifact arising from the mesh granularity (20 nm x 20 nm x 20 nm). Loss is expected to decrease with higher resolution mesh, but this would require computational resources beyond our current capability. In addition, thickness tapering would require the extra fabrication complexity of greyscale lithography.

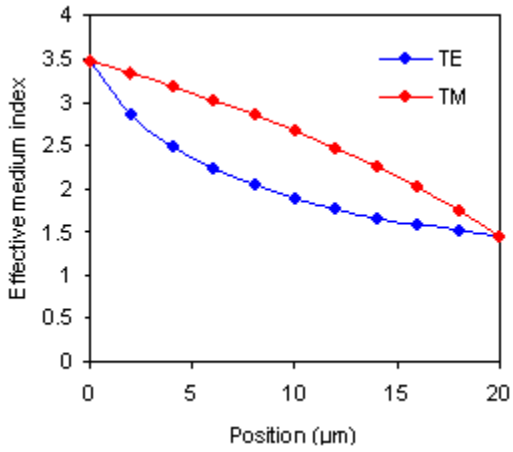

Fig. 3. First order effective medium theory approximation of effective index of SWG upper cladding transition region as a function of position (z in Fig. 1) for TE and TM polarization.

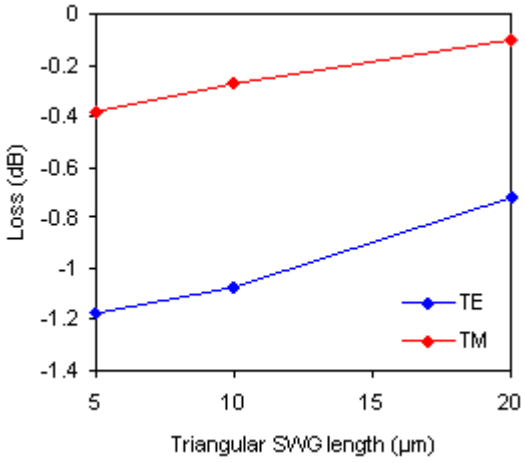

Fig. 4. Loss dependence for triangular SWGs of different lengths. TE and TM polarization, d_A = 1.0 μm, and d_e = 0.4 μm (40% etch). Loss is calculated as power transfer from the fundamental mode of slab waveguide *A* to the fundamental mode of slab waveguide *B* (Fig. 1(b)).

3.1.1 3D FDTD simulation results for TE polarization

Simulation results for TE polarized light at λ = 1.54 μm are shown in Fig. 5, indicating the loss incurred by the power transfer from slab waveguide *A* to the fundamental mode of slab waveguide *B* for d_A = 0.5 μm, 1.0 μm and 1.5 μm with various etch depths (in percentage of the initial slab waveguide thickness). A significant improvement in performance compared to the conventional single-step is present. For example, at initial slab thickness d_A = 1.5 μm (Fig. 5(a)) and etch depth of d_e = 0.6 μm (40% etch) mode coupling loss for a conventional single-step is –2.6 dB. Using the triangular SWG mode transformer, mode coupling loss is reduced to –1.6 dB. The triangular-transverse grating yields a further loss reduction to –1.3 dB. For d_A = 1.0 μm

#112127 - $15.00 USD Received 1 Jun 2009; revised 13 Aug 2009; accepted 15 Aug 2009; published 8 Oct 2009

(Fig. 5(b)), and d_e = 0.4 μm (40% etch) mode coupling loss for a conventional single-step is –2.2 dB. By using the triangular grating, the loss is reduced to –0.7 dB, while with triangular-transverse SWG the loss is further reduced to –0.25 dB. In Fig. 5(b) there is a noticeable discontinuity in the calculated loss for the triangular grating etch depth range 0.4 μm to 0.5 μm, which we attribute to higher order mode excitation at d_e = 0.5 μm. For the 0.5 μm thick SOI slab (Fig. 5(c)) simulation results confirm that both the triangular and triangular-transverse SWGs have improved performance over the conventional single-step, with the triangular SWG having the smallest loss penalty. For the triangular and triangular-transverse mode transformers as d_A increases (0.5 μm, 1.0 μm, 1.5 μm), loss also increases for a given etch percentage. Since increasing d_A creates a larger vertical step (for the same etch percentage), the SWG transition from d_A to d_B is less adiabatic resulting in increased loss.

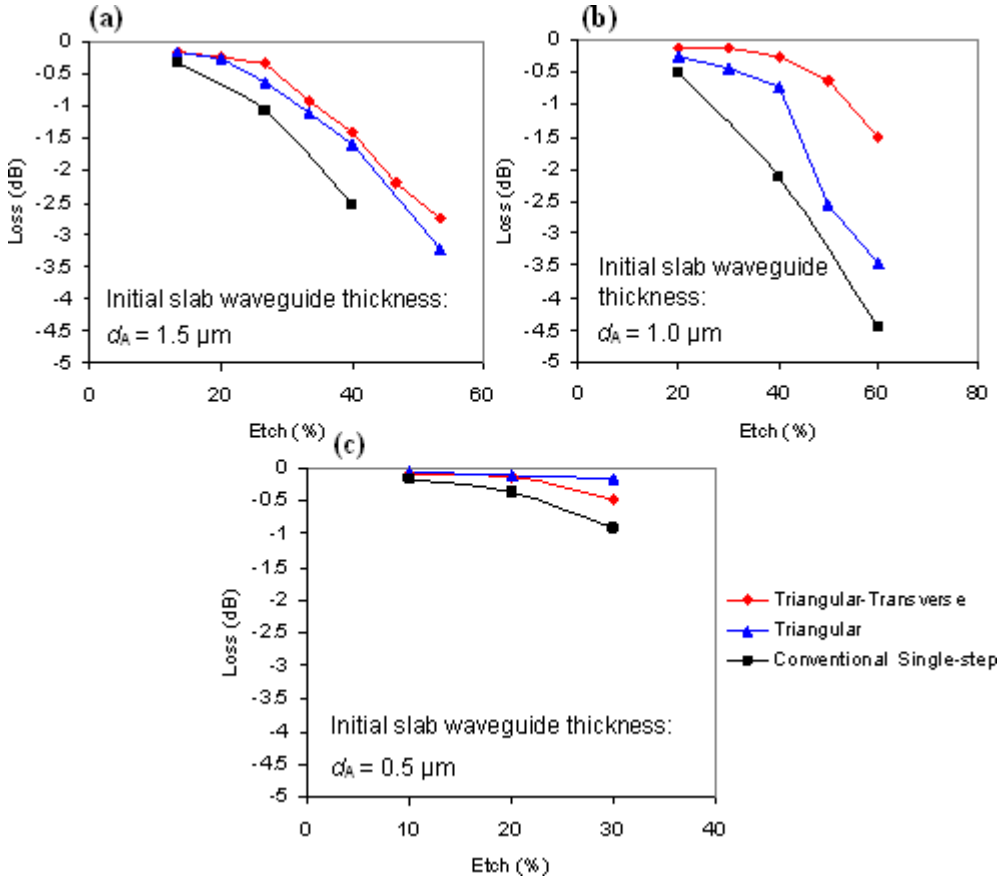

Fig. 5. Vertical mode transformer loss comparison for conventional single-step, triangular SWG and triangular-transverse SWG for TE polarization. a) Initial slab thickness d_A = 1.5 μm, etch depth range d_e = 0.2 μm – 0.8 μm (10% – 50% etch) ; b) d_A = 1.0 μm, d_e = 0.2 μm – 0.6 μm (20% – 60% etch); c) d_A = 0.5 μm, d_e = 0.05 μm – 0.15 μm (10% – 30% etch). Loss is calculated as power transfer from the fundamental mode of slab waveguide *A* to the fundamental mode of slab waveguide *B* (see Figs. 1(b) and 1(c)).

3.1.2 3D FDTD simulation results for TM polarization

Simulation results for TM polarized light at λ = 1.54 μm are shown in Fig. 6, indicating the loss incurred by the power transfer from slab waveguide *A* to the fundamental mode of slab waveguide *B*. Compared to TE polarization, here the trend is reversed, i.e. the triangular SWG

#112127 - $15.00 USD Received 1 Jun 2009; revised 13 Aug 2009; accepted 15 Aug 2009; published 8 Oct 2009

loss is lower than triangular-transverse SWG loss, for all studied initial slab thicknesses d_A. For example at d_A = 1.5 μm (Fig. 6(a)) and etch depth of d_e = 0.6 μm (40% etch) mode coupling loss for a conventional single-step is −1.2 dB. Using triangular-transverse SWG mode transformer, mode coupling loss is reduced to –0.6 dB, while for triangular SWG the loss is as low as –0.2 dB. For d_A = 1.0 μm (Fig. 6(b)), and d_e = 0.4 μm (40% etch) mode coupling loss for a conventional single-step is −3.2 dB. Using the triangular-transverse SWG the loss is reduced to –0.6 dB, while for triangular SWG the loss is as low as –0.1 dB. For the 0.5 μm thick SOI slab (Fig. 6(c)) and d_e = 0.15 μm mode the coupling loss for a conventional single-step is –1.6 dB. The loss is reduced to –0.7 dB and –0.3 dB with triangular-transverse and triangular SWG, respectively. Unlike for TE polarization, loss performance of the triangular SWG is superior to the triangular-transverse SWG. We attribute the excess loss of the triangular-transverse structure to the decreased confinement at the upper cladding boundary for TM polarization (compared to the triangular SWG) that arises from a reduced effective index due to the transverse segmentation. This results in an increased mode mismatch between the thinner slab waveguide (highly confined mode) and the transition region of the triangular-transverse SWG (reduced mode confinement). Amplitude mode profiles at the light output plane (Fig. 2) for d_A = 1.0 μm and d_e = 0.4 μm are shown in Fig. 7 indicating overlap percentage Γ of the fundamental mode. It is observed that the SWG mode transformers have reduced higher order mode excitation compared to the conventional step.

#112127 - $15.00 USD Received 1 Jun 2009; revised 13 Aug 2009; accepted 15 Aug 2009; published 8 Oct 2009

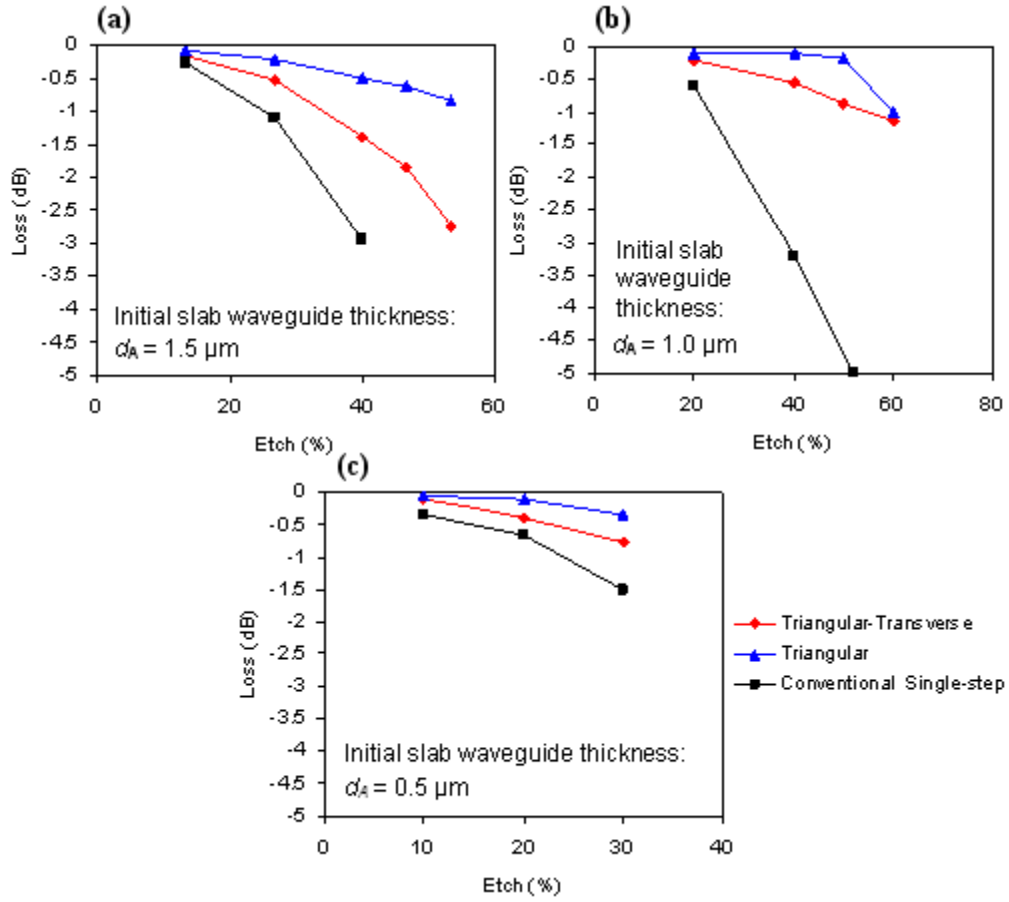

Fig. 6. Vertical mode transformer loss comparison for conventional single-step, triangular SWG and triangular-transverse, SWG for TM polarization. a) Initial slab thickness d_A = 1.5 µm, etch depth range d_e = 0.2 µm – 0.8 µm (10% – 50% etch); b) d_A = 1.0 µm, d_e = 0.2 µm – 0.6 µm (20% – 60% etch); c) d_A = 0.5 µm, d_e = 0.05 µm – 0.15 µm (10% – 30% etch). Loss calculated as power transfer from the fundamental mode of slab waveguide *A* to the fundamental mode of slab waveguide *B* (see Figs. 1(b) and 1(c)).

#112127 - $15.00 USD Received 1 Jun 2009; revised 13 Aug 2009; accepted 15 Aug 2009; published 8 Oct 2009

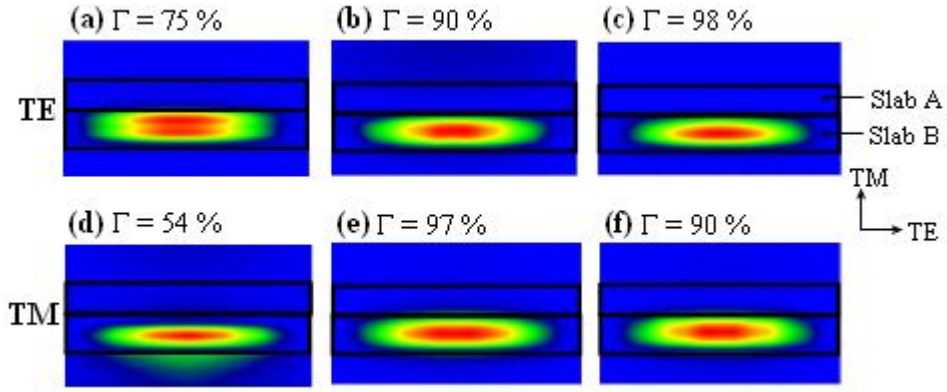

Fig. 7. TE and TM mode profiles for d_A = 1.0 μm and d_e = 0.4 μm. TE polarization: a) Conventional single-step, indicates higher order mode excitation, b) Triangular SWG showing higher mode mismatch than, c) Triangular-transverse SWG. TM polarization: d) Conventional etch indicates significant mode mismatch, e) Triangular SWG showing lower mode mismatch than, f) Triangular-transverse SWG.

3.1.3 SWG mode transformers with reduced polarization dependent loss (PDL)

The simulation results discussed in Sections 3.1.1 and 3.1.2 show that mode coupling loss, for both triangular and triangular-transverse SWGs, is polarization dependent. However, since triangular SWG loss is lower for TM polarization while triangular-transverse SWG loss is lower for TE polarization, a combination of the two types of SWG structures can be used to mitigate PDL. Here we propose two structures with reduced PDL (Fig. 8). The first structure comprises a triangular SWG followed by a triangular-transverse SWG of length L_T, as shown in Fig. 8(a). Figure 9 shows loss for TE and TM polarizations as a function of transverse SWG length L_T for d_A = 1.0 μm, d_e = 0.4 μm (40%) and triangular SWG length of 20 μm. The calculated PDL is negligible for a transverse grating length of 18 μm, where mode coupling loss for TE and TM is ~-0.5 dB. The second approach to reduce PDL is to form a transverse SWG in the region between the triangular teeth as shown in Fig. 8(b). The geometrical parameters of these transverse gratings across continuous triangular structures are Λ_i = 180 nm, Λ_f = 220 nm, a_i = 130 nm and a_f = 50 nm (Fig. 8(b)). Using the same slab etch dimensions as in the structure of Fig. 8(a), simulation results show mode coupling loss for TE and TM is –0.2 dB and –0.38 dB, respectively. The advantage of this structure compared to partial transverse SWG is a decreased overall loss, but some residual PDL < 0.2 dB remains. We believe the latter may still be reduced by further optimization.

#112127 - $15.00 USD Received 1 Jun 2009; revised 13 Aug 2009; accepted 15 Aug 2009; published 8 Oct 2009

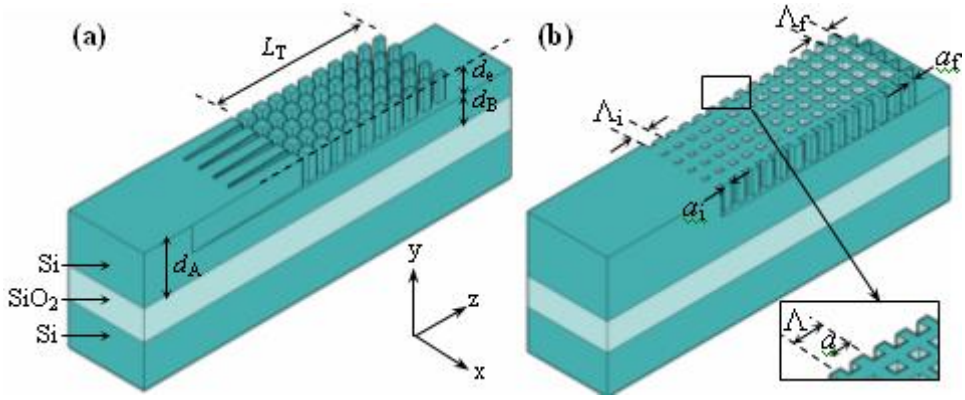

Fig. 8. 3D mode transformers with reduced PDL. a) Partial transverse SWG with length L_T; b) Transverse SWG in the region between the triangular teeth.

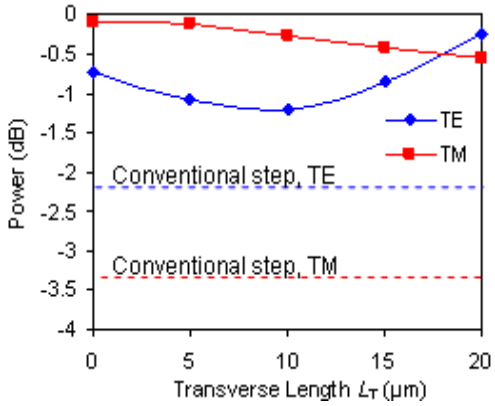

Fig. 9. Power coupled to the fundamental mode for a structure shown in Fig. 8(a). Negligible PDL is predicted for triangular-transverse length L_T ~18 μm. Dotted lines indicate the loss for a conventional step for TE and TM polarization, respectively.

3.2 SWG boundary between a slab waveguide and a waveguide array

To explore other potential applications of SWG mode transformers, we use sub-wavelength gratings to reduce the mode mismatch between the slab waveguide combiner and the waveguide array of an AWG. The main intrinsic source of loss in an AWG is coupling from the slab waveguide to the waveguide array. This loss is a consequence of different field distributions of the slab waveguide and the arrayed waveguides. As the continuous field in the slab waveguide propagates across the slab-array boundary, it couples to the discretized field of the array of waveguides. Here loss is particularly significant in high index contrast waveguides as the strong confinement results in increased reflection and mode mismatch. This effect can be reduced by optimizing the slab-array interface; for example, loss < 0.4 dB has been reported by employing a double-etch process [22]. Deep etched waveguides in the array are adiabatically tapered to shallow etched regions near the slab to create a gradual index transition; however, this implies increased fabrication complexity. Figure 10 shows an AWG schematic with a close-up of the slab-array boundary. Two structures are compared, namely a conventional taper (Fig. 10(a)) and a SWG taper (Fig. 10(b)). The latter is used to create an effective medium gradually matching the slab effective index to that of the waveguide array. Figures 11(a) and 11(b) show the layout dimensions of 2D FDTD simulations with a grid of $\Delta x \times \Delta y = 10 \times 10$ nm^2. Figures 11(c) and 11(d) show the field evolution along a conventional taper and a SWG taper. It is

#112127 - $15.00 USD Received 1 Jun 2009; revised 13 Aug 2009; accepted 15 Aug 2009; published 8 Oct 2009

observed that higher order mode excitation is significantly suppressed for the SWG boundary. Figures 11(e) and 11(f) show the field amplitude profile in the array waveguides. Conventional taper loss is −1.4 dB, while using SWG structure loss is markedly reduced, to < −0.2 dB.

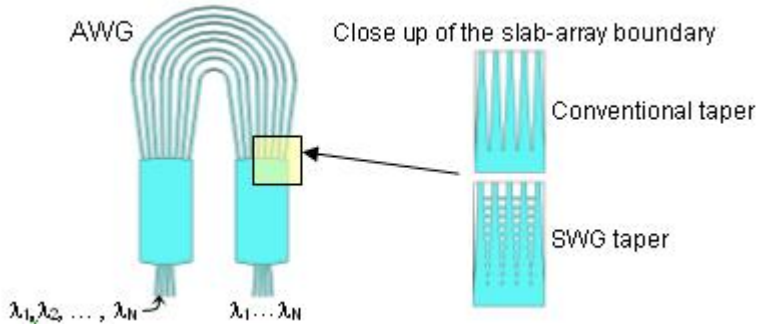

Fig. 10. AWG with close-up of the slab-array boundary using conventional tapers and SWG tapers to reduce loss and higher order mode excitation at the slab-array boundary.

In our SWG taper slab-array boundary, diffraction is frustrated as the grating period is less than the first order Bragg period, unlike in mode transformer proposed for the low index contrast silica-on-silicon waveguide platform using a long period grating (LPG) [23]. Application of LPGs to a high contrast waveguide platform such as SOI is limited due to the prohibitive losses incurred at the interfaces between different LPG segments.

#112127 - $15.00 USD Received 1 Jun 2009; revised 13 Aug 2009; accepted 15 Aug 2009; published 8 Oct 2009

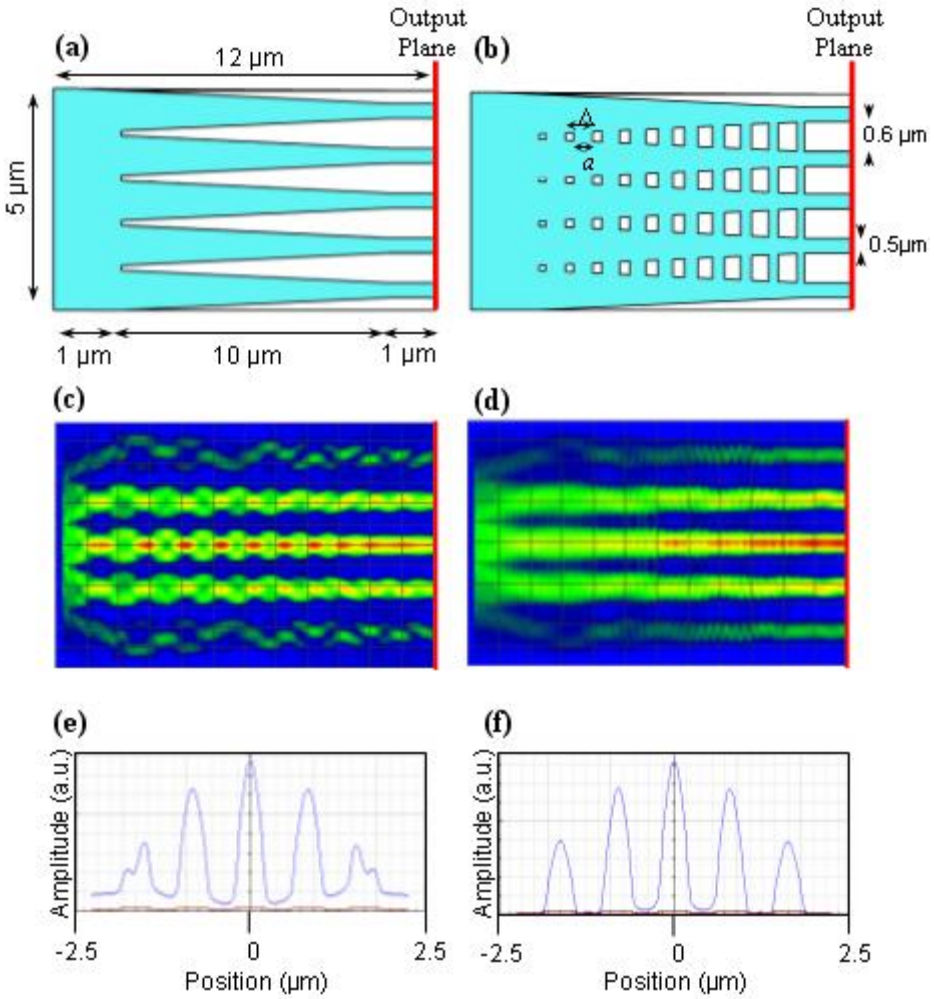

Fig. 11. Layout, mode evolution and field profiles for an AWG slab-array boundary. a) Conventional taper simulation layout. b) SWG taper simulation layout. c) Field evolution in conventional tapers, higher order mode excitation is noticeable. d) Field evolution in SWG taper with suppressed higher order mode excitation. e) Conventional taper field amplitude profile at the output plane of the waveguide array indicating the presence of higher order modes. f) SWG taper field amplitude profile at the output plane of the waveguide array indicating suppressed higher order mode excitation.

4. Conclusion

We proposed and studied by 3D FDTD simulations several new sub-wavelength grating mode transformers for mode coupling between high refractive index contrast (SOI) waveguides of different geometries, including different waveguide core thicknesses and a junction between a slab waveguide and a waveguide array. Compared to conventional structures, our mode transformers significantly reduce loss, PDL and higher order mode excitation. For vertical mode transformers, the loss compared to a conventional step etch is reduced by up to 3 dB depending on the specific waveguide geometry, and PDL can be effectively mitigated. Using a SWG boundary between a slab waveguide and a waveguide array in a photonic wire AWG, a significant loss reduction from –1.4 dB to < –0.2 dB and a reduced higher order mode excitation

#112127 - $15.00 USD Received 1 Jun 2009; revised 13 Aug 2009; accepted 15 Aug 2009; published 8 Oct 2009

are predicted. An important practical advantage of these sub-wavelength grating mode transformers is that they can be fabricated in a single etch step.

#112127 - $15.00 USD Received 1 Jun 2009; revised 13 Aug 2009; accepted 15 Aug 2009; published 8 Oct 2009